Radiation Physics and Chemistry 223 (2024) 111873

Contents lists available at ScienceDirect

Radiation Physics and Chemistry

journal homepage: www.elsevier.com/locate/radphyschem

Enhancing radiation-hardness of Si-based diodes: An investigation of Al-doping effects in Si using I–V measurements

D.A. Oeba [a], J.O. Bodunrin [b,*], S.J. Moloi [b]

[a] Department of Physics, Faculty of Science, Egerton University, P.O Box 536-20115, Egerton, Kenya
[b] Department of Physics, College of Science, Engineering and Technology, University of South Africa, Private Bag X6, Florida, 1710, South Africa

ARTICLE INFO

Handling Editor: Chris Chantler

Keywords:
Silicon diode
Current
Conduction mechanisms
Proton irradiation
Radiation suppression
Radiation detectors

ABSTRACT

The impact of radiation on Si-based detectors garnered interest due to the observed degradation in their stability in high-radiation environments. In this study, we examined the effects of 3 MeV proton irradiation on both undoped and Al-doped *n*-Si diodes using *I–V* technique. The results revealed a decline in current trends for both types of diodes post-irradiation. This decrease was attributed to defects created by proton irradiation, which acted as recombination or trapping centres. However, the Al-doped *n*-Si diodes experienced a lesser decline in measured current, hinting at the radiation suppression effect of Al doping in Si. Additionally, Al-doped *n*-Si diodes displayed minimal changes in their diode parameters after irradiation, and their conduction mechanism remained unchanged. These results suggested that Al-doped *n*-Si diodes had superior stability compared to their undoped counterparts, implying that the presence of Al enhanced the diodes' resistance to radiation. The radiation suppression effect of Al seemed to stem from its ability to produce defects that improve Si's radiation-hardness, thereby mitigating the introduction of additional instability-causing defects during proton irradiation. Thus, incorporating Al was recommended for research aiming to improve the radiation resistance of Si.

1. Introduction

For many decades, Si has been used extensively for the fabrication of radiation detectors for nuclear medicine, high energy physics experiments, and lasers in military operations (Rosenfeld, 2006; Terzo et al., 2017). Also, Si material is used in the fabrication of the Schottky diodes for radiation sensing applications due to its advantages over other semiconductor. These advantages include low cost due to its abundance in nature, well-known technology as a result of long-term studies, and presence of natural oxide layer to mention a few. Furthermore, the structure of Schottky diodes enables low-temperature processing for fabrication (Terzo et al., 2017). In this way, factors associated with high temperature such as impurity diffusion and impurity activation after ion implantation can be avoided in the fabrication process. These diodes are distinguished by their quick signal response, high inherent detection efficiency, low operational voltage, and improved energy resolution (Rosenfeld, 2006; Terzo et al., 2017; Moloi and McPherson, 2009a). However, it has been observed that prolonged use of Si-based detectors under harsh environment causes degradation in their efficiency during operation as a result of low charge collection efficiency, high leakage current, and high depletion voltage (Van Lint, 1987; Thebe et al., 2021).

Past studies have shown that a viable way of improving radiation-hardness of Si material involves doping Si with metals such as gold (Au) and platinum (Pt) (Dixon and Ekstrand, 1986; Bodunrin and Moloi, 2022). This improvement in Si's radiation-hardness is attributed to the defect levels induced close to the centre of the band gap of Si (≈0.56 eV) (Bodunrin and Moloi, 2022). However, other defects induced by Au and Pt in Si affects the conductivity of the material (Dixon and Ekstrand, 1986; Bodunrin and Moloi, 2022). Also, these metals are expensive and not easily available for research; hence, there is a need for alternative dopants that are economical and still capable of producing similar effects as Au and Pt in Si.

Al could be a possible alternative dopant to the established Au and Pt in Si for improvement of radiation-hardness of Si (Krause et al., 2002; Rosenits et al., 2007; Chen and Milnes, 1980; Nevin and Henderson, 1975; Lee et al., 1980). For example, Al is an acceptor dopant in Si to fabricate power semiconductor devices with a *p-n* junction (Krause et al., 2002). According to Rosenits et al. (2007), doping Si with Al induces shallow and deep defect levels at E_V +0.057 eV and E_V +0.44 eV, respectively. Moreover, an investigation into the thermal properties of Al-doped Si revealed deep levels following heat treatment, as assessed by thermally stimulated capacitance (TSCAP) measurements (Chen and

* Corresponding author.
E-mail address: ebodunjo@unisa.ac.za (J.O. Bodunrin).

https://doi.org/10.1016/j.radphyschem.2024.111873
Received 17 January 2024; Received in revised form 8 May 2024; Accepted 24 May 2024
Available online 28 May 2024

Milnes, 1980). Specifically, three hole traps, each exhibiting concentrations in the range of 10^{12}–10^{14} cm^{-3}, were identified at energy levels E_V +0.216, E_V +0.316, and E_V +0.402 eV. Additionally, an electron trap with a concentration of 10^{13} cm^{-3} was observed at E_C− 0.39 eV. These findings are ascribed to the intricate formation of pairs or complexes involving Al and oxygen (O) atoms within the Si lattice. Profiling measurements further indicate that a phosphorus n + layer serves as a recombination centre for Al–O complexes.

In a parallel investigation, deep levels at E_V +0.43, and E_V +0.47 eV were documented in an Al-doped Si ingot (Nevin and Henderson, 1975). Also, Al in Si has been found to create acceptor levels at E_V +0.55 eV (Lee et al., 1980). This comprehensive exploration enhances our understanding of the intricate interplay between Al and Si, shedding light on the nuanced energy levels and interactions that occur within the material. The Al-induced acceptor levels (or electron trap) are responsible for generating holes in Si that recombines with electrons in *n*-Si to decrease the density of free charge carriers, hence an increase in the material resistivity. Si detector fabricated on resistive material has been found to be tolerant to radiation damage (Van Lint, 1987; Thebe et al., 2021; Dixon and Ekstrand, 1986). The defect level at 0.55 eV induced by Al is close to the centre of bandgap of Si and identical to that induced by Au and Pt, which is responsible for the radiation-hardness of the Si material (Dixon and Ekstrand, 1986); hence, there is a motivation for investigating the effect of Al on the electrical properties of Si-based diode.

This study aims to investigate how the introduction of Al affects the electrical properties of Si-based diodes. Additionally, it seeks to determine whether Al has a suppressive effect on irradiation damage. The study utilizes *I–V* characteristics to analyse diode behaviour before and after proton irradiation in both undoped and Al-doped *n*-Si materials. The research examines changes in diode parameters, including the ideality factor, saturation current, Schottky barrier height (SBH), series resistance, shunt resistance and rectification ratio (RR), based on the collected *I–V* data.

2. Experimental details

2.1. Sample preparation

Semiconductor Wafer Inc. manufactured the *n*-Si wafer used in this study. The *n*-Si wafer has a thickness of 275 ± 25.0 μm and resistivity varying from 1 to 20Ω.cm. The wafer was cut into pieces of 0.6 cm by 0.6 cm. The parts were cleaned in accordance with industry standards to get rid of handling grease and other contaminants, and they were then submerged in a 40% HF solution to get rid of the surface layer of oxygen (Vittone et al., 2005). The doping was carried out at iThemba LABS in Gauteng, South Africa, utilising an ion implanter setup. At a 160 keV energy and 1.0 × 10^{17} ion cm^{-2} fluence, Al was implanted onto the polished side of the Si wafers. The setup's maximum attainable setting of 160 keV and 1.0 × 10^{17} ion cm^{-2} was chosen in order to generate as many deep defects in Si as possible (Dixon and Ekstrand, 1986). Before ion implantation, Stopping and Range of Ions in Matter (SRIM) 2013 software was used to estimate the Al's predicted range and maximum implantation depth, which were ~270.7 and 550 nm, respectively. It was hypothesised that the energy of 160 keV would be sufficient to generate defects in Si based on the data collected from SRIM.

2.2. Diode fabrication

Schottky-based diodes (SBDs) were fabricated on both undoped and Al-doped *n*-Si. The samples were cleaned once more to get rid of handling grease and contaminants before being blow-dried with nitrogen gas to make the ohmic and Schottky contacts. The ohmic contact was realized by thermally evaporating Al onto the whole backside of the *n*-Si wafers with 100 nm thicknesses. In order to improve the ohmic contact, the samples were annealed at 375 °C for 40 min in a vacuum. The annealing was done to optimize the ohmic contact and reduce resistivity at the back contact. For the Schottky contact, Au was deposited on the polished side of the *n*-Si with 130 nm thickness through a mask with 0.6 mm radius holes. The deposition took place at a rate of 1 A s^{-1} at 10^{-6} mbar. The schematic diagram of the fabricated SBD is presented in Fig. 1.

2.3. Device irradiation

SBDs were irradiated with 3 MeV protons. The proton-irradiation was carried out using an ion implanter located at iThemba LABS, Gauteng Province, South Africa. Prior to irradiation, the beam fluence φ was estimated from the irradiated time (*t*), beam current (*I*), and the beam spot area (*B*) on the target (Song et al., 2003) as

$$\varphi = \frac{It}{qeB} \tag{1}$$

where *q* is the ionic charge and *e* is the electron charge. After several trials with different values of *t*, it was realized that an average beam current of 5 nA and irradiation time of 10 h is needed to achieve a fluence of 10^{17} ion cm^{-2}. This fluence was chosen to provide the highest damage to the device. The beam current was monitored and recorded for the duration of each irradiation. This was necessary to ensure that the beam current remains constant to maintain the same fluence for all the samples. The samples were labelled as follows before diode characterization.

(i) Unirradiated undoped *n*-Si diode as unirra *n*-Si SBD (D1)
(ii) Proton-irradiated undoped *n*-Si diode as irra *n*-Si SBD (D1i)
(iii) Unirradiated Al-doped *n*-Si diode as unirra *n*-Si SBD (D2)
(iv) Proton-irradiated Al-doped *n*-Si diode as irra Al-*n*-Si SBD (D2i)

2.4. Diode characterization

I–V data was collected at 300 K and under dark conditions. The *I–V* measurement was done at voltage range of −3 to 3 V. These voltages were chosen to eliminate effects of thermionic emission current that is active at low voltages (below ~0.7 V for Si.) (Yüksel et al., 2008; Güllü et al., 2008a). A program in LabVIEW was developed to enable readings from an in-house-made meters linked to the probe station. By magnifying the device with a microscope, the precise connection between the device and the probe was ascertained. A metallic shield was used to encase the test fixture, serving the dual purpose of isolating the measurement system from external electromagnetic fields and maintaining a dark environment within the probe station.

3. Results and discussion

Fig. 2 shows *I–V* characteristics of D1 and D1i in a semilogarithmic

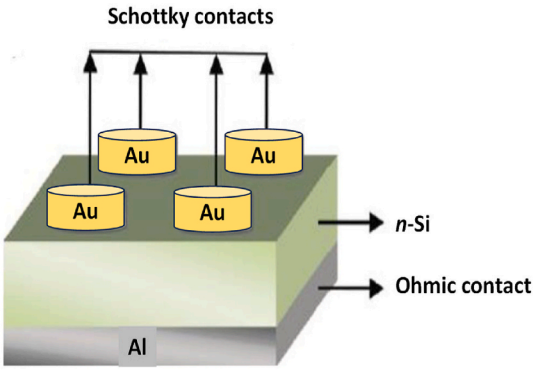

Fig. 1. Schematic diagram of Au/n-Si SBD.

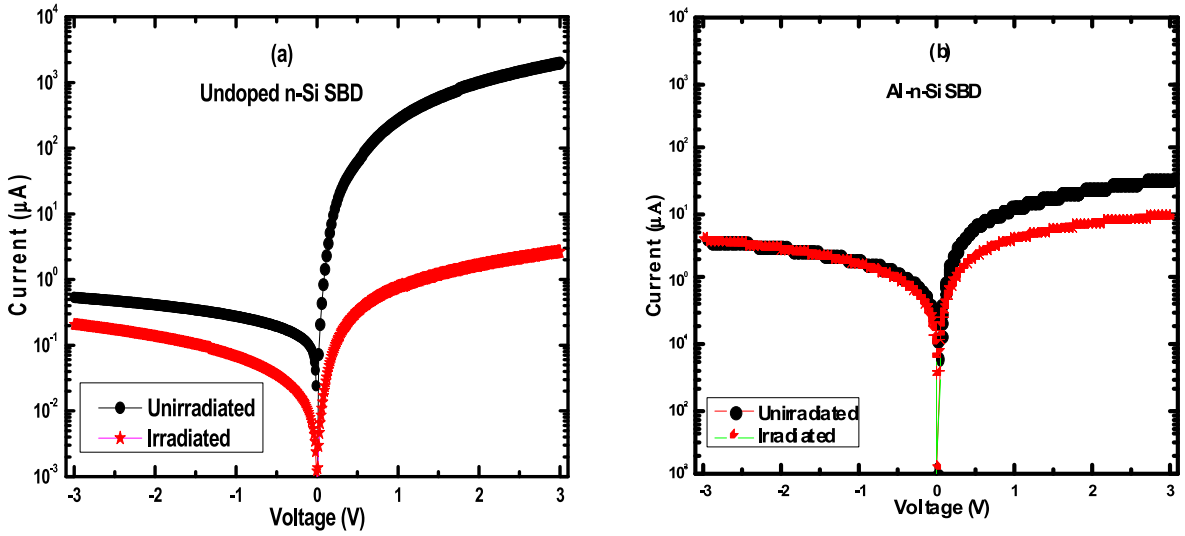

Fig. 2. I–V characteristics of unirradiated and proton-irradiated undoped (a) and Al-doped (b) n-Si SBD in semi-logarithmic scale.

scale. As observed in Fig. 2 (a), diodes show a linear increase in forward current at low voltages but a deviation from linearity at high voltages, demonstrating the effects of series resistance (R_s) (Thebe et al., 2021). The reverse and forward currents decrease after proton irradiation with the forward current decreasing more, suggesting that radiation-induced defects recombine more with the majority carriers (electrons) than the minority carriers (holes). The recombination of the charge carriers leads to a low charge carrier density in the space charge region (SCR). This finding is consistent with reports in the literature (Casse et al., 2000; Gurimskaya et al., 2020) based on neutron- and proton-irradiated diodes, implying that radiation-induced defects recombine with charge carriers in Si material.

Fig. 2 (b) shows *I–V* characteristics of D2 and D2i in a semi-logarithmic scale. The reverse current of the D2 and D2i shows insignificant change, indicating that the reverse current is not affected by proton irradiation. The insignificant change observed could be as a result of the Al-induced defects restricting the further generation of radiation-induced minority carriers (holes) responsible for reverse current. This observation shows that Al in Si improves the stability of the devices to incident particles. It should be noted that radiation detectors are best operated in the reverse bias conditions because they offer advantages such as reduced dark current, improved signal-to-noise ratio, lower capacitance, enhanced quantum efficiency, and avoidance of saturation, making it a preferred configuration for many types of detectors in various applications (Sze et al., 2021). Upon irradiation, on the other hand, the forward trend shifts down like that observed on undoped diode, indicating that current has decreased after proton irradiation. However, the decrease in current has reduced sufficiently, confirming that the effect of radiation on forward current has been supressed. Further analysis of the D2 and D2i reveal that the effects of radiation on the device are greatly minimized and there is a complete suppression on reverse current, indicating that Al is a suitable dopant in improving radiation-hardness of Si. The improved radiation-hardness is as a result of Al-induced defects hindering the further dislodgement of atoms by incident radiation, making the crystal structure stable and independent of incident energetic particles.

According to thermionic emission theory (Gurimskaya et al., 2020), current I through a diode is given as

$$I = I_S\left[\exp\left(\frac{eV - IR_s}{\eta kT}\right)\right]. \tag{2}$$

The saturation current (I_S) is determined from the straight linear fitting of the forward ln(*I*)–*V* plot at zero bias and is expressed (Güllü et al., 2008a) as

$$I_S = AA^*T^2\left(\frac{-e\Phi_b}{kT}\right) \tag{3}$$

where, A is the area of the diode, A^* is the Richardson constant equivalent to 112 $Acm^{-2}K^{-2}$ for *n*-type Si at room temperature, and Φ_b is the SBH. The ideality factor, η, is calculated by replacing the slope of the linear region of the forward ln(*I*)–*V* characteristic in

$$\eta = \frac{e}{kT}\frac{dV}{d(\ln I)} \tag{4}$$

where, $\frac{dV}{d(\ln I)}$ is $\frac{1}{\text{slope}}$ of the linear region of ln(*I*)–*V* graph. The ideality factor of an ideal diode is 1, but in practice its more than 1 (Sevgili, 2021). $\eta > 1$ shows additional current mechanism other than thermionic emission become involved. The I_S evaluated from Eq. (3) is used to calculate the SBH as

$$\Phi_b = \frac{kT}{e}\ln\left(\frac{AA^*T^2}{I_S}\right). \tag{5}$$

The values of series resistance (R_s) and shunt resistance (R_{sh}) for the fabricated diodes were derived from the junction resistance versus voltage ($R_j - V$) plot shown in Fig. 3. In reverse bias, the maximum R_j value corresponds to R_{sh}, while the minimum R_j value at sufficiently high forward voltage corresponds to R_s. These values are tabulated in Table 1. As depicted in Fig. 3 and Table 1, a more significant change is observed in R_s values compared to R_{sh} values following proton irradiation. This phenomenon may be attributed to the defects induced by proton irradiation, which tend to recombine or trap more electrons than holes. A notable change in R_{sh} for Al/(ZnO-PVA)/*p*-Si type Schottky diodes under gamma-irradiation is available in literature (Kaymaz et al., 2021). The alteration in R_{sh} and R_s is attributed to radiation-induced defects, as trap levels can either decrease or increase the free carrier density in the structures, leading to a decrease or increase in the diode's resistance (Kaymaz et al., 2021; Tian and Cao, 2016).

Electrical parameters extracted from the linear section of the semi-logarithmic scale of undoped and Al-doped *n*-Si SBDs before and after proton irradiation are given in Table 1.

For D1, the ideality factor of 1.17, surpassing unity, suggests the presence of additional conduction mechanisms beyond thermionic emission, possibly involving a tunnelling mechanism. This might be due to the SiO_2 layer that forms between Au and Si, resulting in charge carriers recombining through interface states (Sevgili, 2021). Further evidence is provided by the η values of 1.12 and 1.17 observed in

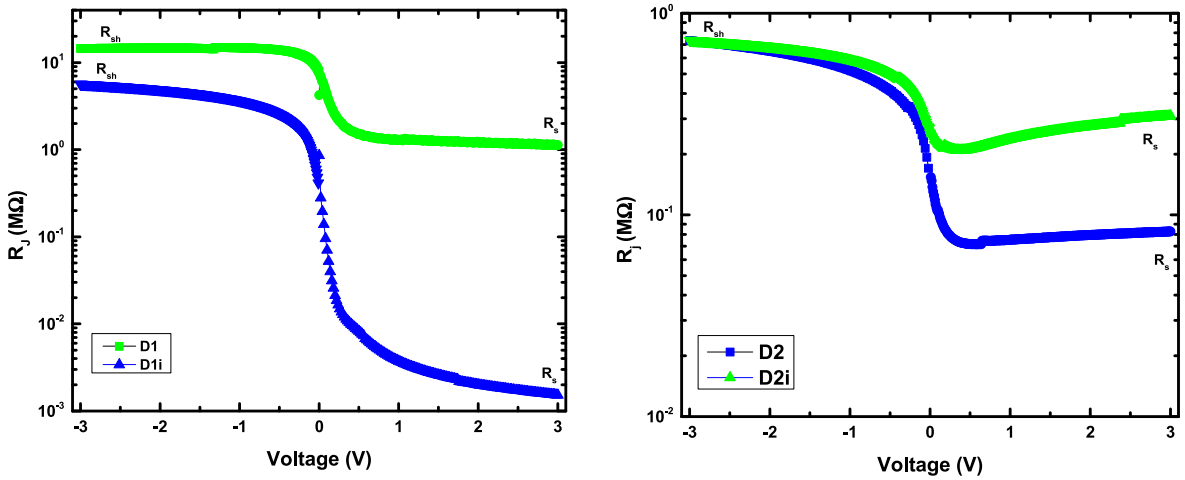

Fig. 3. R_j-V characteristics of unirradiated and proton-irradiated undoped (a) and Al-doped (b) n-Si SBD in semi-logarithmic scale.

Table 1
Diode parameters of the unirradiated and irradiated SBDs calculated using ln*I-V* method.

Diodes		η	φ_b *(eV)*	I_s (nA)	R_{sh} *(MΩ)*	R_s *(MΩ)*	RR
Undoped *n*-Si	**Unirradiated (D1)**	1.17	0.73	18.80	6.04	0.001	3135.09
	Irradiated (D1i)	1.89	0.79	1.74	15.61	1.04	13.53
Al-doped *n*-Si	**Unirradiated (D2)**	3.87	0.67	191.10	0.76	0.07	8.48
	Irradiated (D2i)	3.41	0.70	53.7	0.76	0.20	2.32

Au/*n*-Si diodes with metal-Si interface layers of 1.5 nm and 2.5 nm thickness, respectively (Reddy and Reddy, 2012). For D1i, the η value is 1.89, higher than 1.17 evaluated on D1. A higher η highlights the influence of a generation-recombination (*g-r*) charge distribution due to radiation-induced *g-r* centres, which act as traps or recombination centres (Thebe et al., 2021; Bodunrin and Moloi, 2022),resulting in an increase in resistivity due to a reduced charge carrier density within the SCR.

In the case of the D2, the η value increased to 3.87 from the 1.17 of D1. This suggests Al-doping introduces another conduction mechanism, possibly the *g-r* mechanism, due to Al-induced defects in Si's bandgap. Post-irradiation (D2i), the η value is 3.41, comparable to the 3.87 of D2, indicating Al has mitigated the effects of irradiation, leading to a more stable Al-doped diode. The η for D1 has increased due to an involvement of charge distribution method in the material due to radiation induced *g-r* centres. *G-r* centres act as traps or recombination centres increasing the resistivity of the material. An increase in the resistivity is as a result of a decrease in the charge carrier density in the SCR. The η for D2i has decreased slightly, indicating an improved diode's quality due to reduced non-ideal behaviour post-proton irradiation. This observation suggests that the irradiation's effect on D2 has diminished, potentially enhancing the radiation hardness of Si material.

The φ_b of D1 (0.73 eV) is within the range of reported values: lower than the 0.75 eV for Sn/*p*-Si (Hanselaer et al., 1986) but higher than the 0.63 eV for Au/*p*-Si (Moloi and McPherson, 2009b). This confirms the effective fabrication of our diodes. It's observed that irradiation induces bandgap defects affecting carrier concentration, resulting in a φ_b increase for *n*-type semiconductors (Güllü et al., 2008b). Hence, in our study, proton irradiation-induced defects reduce the carrier concentration in the SCR, increasing the φ_b post-proton irradiation. For D2, φ_b decreases to 0.67 eV from the D1's 0.73 eV. This decreases post-Al-doping suggests Al-induced defects generate carriers within the SCR. After irradiation, though φ_b did increase, the magnitude of change was smaller compared to the *n*-Si diode, signifying enhanced stability in Al-doped diodes.

The I_s for D1 is 18.80 nA, which is within the acceptable range, considering its higher than the 10.00 nA for Au/ZnO thin film SBDs on Si (Rajan et al., 2016), but lower than the 160.00 nA for Si PIN diodes (Parida et al., 2018). Post-proton irradiation, I_s decreases due to trapping and recombination of carriers from irradiation-induced defects, a phenomenon also observed in gamma-irradiated *p*-Si-based diodes (Güllü et al., 2008c). For D2, I_s significantly increases post-Al doping, indicating Al-induced defects introduce minority carriers raising I_s. Although I_s reduces after proton irradiation, the decrease is less pronounced in the Al-doped diode compared to the undoped diode, revealing Al-doping provides stability against the irradiation.

The values of R_{sh} and R_s for D1 are 6.04 and 0.001 MΩ, respectively, displaying a significant difference that confirms the rectification behaviour of the fabricated diode. Following irradiation, both R_{sh} and R_s increased, indicating that proton irradiation increasess diode resistance due to the trapping and recombination of carriers by irradiation-induced defects. For D2, R_{sh} decreases after Al doping, suggesting that Al-induced defects introduce minority carriers, while R_s increases due to the recombination of majority carriers resulting from Al doping. After irradiation, the disparity in R_{sh} and R_s values are relatively smaller in D2 compared to D1, affirming the suppressive effect of Al on irradiation.

Upon irradiation, the rectification ratio (RR), a ratio of the forward current to the reverse current at 3 V, of *n*-Si SBD drastically reduces from 3135.09 to 13.53. In contrast, the RR of Al-*n*-Si SBD diminishes from 8.48 to 2.32, a relatively smaller decrease. This minimal reduction in the Al-*n*-Si SBD's RR suggests that Al effectively counters radiation's adverse effects, making it a potent dopant to enhance Si's radiation-hardness.

In Fig. 4, the forward *I–V* characteristics of undoped and Al-doped *n*-Si diodes before and after radiation are depicted in logarithmic scale. This figure illustrates the effect of proton irradiation on the conduction mechanism of the fabricated diodes. In Fig. 3 (a), three distinct linear regions are identified as i, ii, and iii on D1. Their respective slopes are 1.85, 2.62, and 1.98. According to references (Missoum et al., 2016; Kaya et al., 2016), a slope of two or above suggests that the predominant charge distribution mechanism is the Space Charge Limited Current (SCLC) which is associated with exponentially distributed surface states. As the applied voltage is increased, the SCLC process leads to the

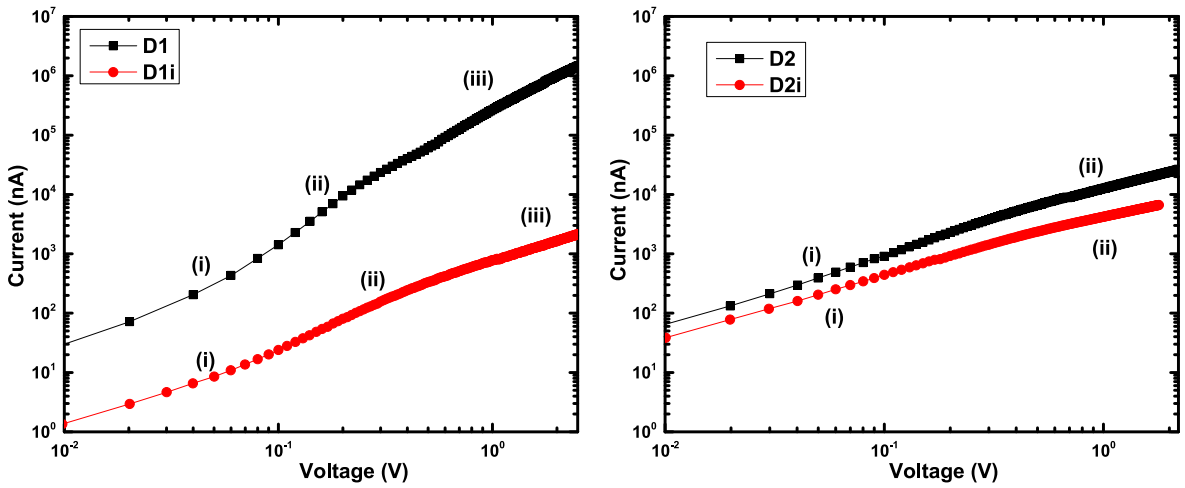

Fig. 4. Current-voltage characteristics of unirradiated (a) and proton irradiated (b) n-Si SBDs in a logarithmic scale.

injection of charge carriers from the electrode into the interface layer (Kaya et al., 2016).

In contrast, D1i, as shown in Fig. 4 (a), presents linear regions with slopes of 1.21, 1.68, and 1.14, respectively. Slopes approximating one indicate that ohmic conduction is the principal mode of conduction. This is attributed to the SCR current surpassing the current produced by the injected free carriers, as elucidated in references (Missoum et al., 2016; Kaya et al., 2016). The reduction in injected carrier concentration from the material into the SCR is due to defects introduced by proton irradiation. The increased resistivity of the material can be attributed to the recombination of charge carriers with radiation-induced defect levels and a decrease in carrier density.

Fig. 4 (b) presents a comparison between the logarithmic *I–V* characteristics of both D2 and D2i. From the linear regions observed in Fig. 3 (b), the derived slope values were 1.12 for region (i) and 0.92 for region (ii) in the D2. Notably, these slope values are close to unity, indicating T that the primary conduction mechanism is ohmic conduction, consistent with previous findings (Bodunrin et al., 2020; Moloi and McPherson, 2009b; Lindström et al., 2001). This ohmic behaviour is attributed to defect levels induced by Al-doping, which introduces generation-recombination (*g-r*) centres, defect levels close to the centre of the bandgap. Such defects engage equivalently with both the conduction and valence bands (Bodunrin et al., 2020; Moloi and McPherson, 2009b; Lindström et al., 2001). The slope of the linear regions in Fig. 4 (b) for the D2i was calculated to be 1.09 and 0.87 for regions (i) and (ii), respectively. Slopes almost unity indicating that the principal conduction mechanism remains ohmic after portion irradiation. Hence, the conduction mechanism remains unchanged after portion irradiation, confirming the suppression effect of Al-doping.

4. Conclusion

I–V characterization technique was used to investigate the electrical properties of undoped and Al-doped *n*-Si-based SBDs prior to and after proton irradiation at ambient temperature. This method offers crucial details regarding the nature of the fabricated diodes, the impact of Al and radiation on the material's electrical characteristics. D1 exhibited rectification behaviour confirmed by R_{sh} and R_s values of 6.04 and 0.001 MΩ, respectively, with both values increasing post-irradiation, indicating heightened diode resistance. In contrast, for D2, R_{sh} decreased after Al-doping, suggesting the introduction of minority carriers due to Al-induced defects, while R_s increased due to majority carrier recombination from Al-doping. The RR of D1 drastically reduced from 3135.09 to 13.53 upon irradiation, whereas the RR of D2 diminished from 8.48 to 2.32, indicating a smaller decrease and highlighting Al's suppressive effect on irradiation. Additionally, the increase in η in D1i suggested the influence of a *g-r* charge distribution due to radiation-induced *g-r* centres, leading to increased resistivity. The decrease in φ_b after Al-doping for D2 and its lesser increase post-irradiation compared to D1 indicated enhanced stability in Al-doped diodes, showcasing Al's potential as a dopant to improve Si's radiation hardness in semiconductor devices. Also, the diode conduction mechanism remains consistent after proton-irradiation of D2. These observations show that the effects of radiation on D2 is greatly minimized and there is a complete suppression on reverse current, indicating that Al is a suitable dopant in improving radiation-hardness of Si. As a result, this metal can serve as an affordable replacement for costly dopants like Au and Pt.

Ethics approval

Not applicable.

Consent to participate

Not applicable.

Consent for publication

We authors give the consent to publish this work.

Availability of data and materials

Not applicable.

Please include the sub-sections below of compliance with ethical standards section

Not applicable.

Research involving human participants and/or animal

Not applicable.

Informed consent

Not applicable.

CRediT authorship contribution statement

D.A. Oeba: Writing – original draft, Methodology, Investigation,

Formal analysis. **J.O. Bodunrin:** Writing – review & editing, Investigation, Formal analysis. **S.J. Moloi:** Writing – review & editing, Supervision, Methodology, Funding acquisition, Conceptualization.

Declaration of competing interest

The authors declare that they have no known competing financial interests or personal relationships that could have appeared to influence the work reported in this paper.

Data availability

No data was used for the research described in the article.

Acknowledgement

This research was fully sponsored by the National Research Foundation of South Africa (Grant numbers 105292 and 114800).

References

Bodunrin, J.O., Moloi, S.J., 2022. Electrical properties and conduction mechanism of heavily implanted iron. Solid State Commun. 341, 114575.
Bodunrin, J.O., Oeba, D.A., Moloi, S.J., 2020. Current-voltage characteristics of iron-implanted silicon based Schottky diodes. Mater. Sci. Semicond. Process., 105524
Casse, G., Allport, P.P., Hanlon, M., 2000. Improving the radiation hardness properties of silicon detectors using oxygenated n-type and p-type silicon. IEEE Trans. Nucl. Sci. 47, 527.
Chen, J.W., Milnes, A.G., 1980. Energy levels in silicon. Annu. Rev. Mater. Sci. 10, 157–228.
Dixon, R.L., Ekstrand, K.E., 1986. Gold and platinum doped radiation resistant silicon diode detectors. Radiat. Protect. Dosim. 17, 527–530.
Güllü, Ö., Çankaya, M., Biber, M., Türüt, A., 2008a. Gamma irradiation-induced changes at the electrical characteristics of organic-based Schottky structures. J. Phys. D Appl. Phys. 41, 135103.
Güllü, Ö., Cimilli, F. Demir F.E., Biber, M., 2008b. γ-Irradiation induced changes at the electrical characteristics of Sn/p–Si Schottky contacts. Vacuum 82, 789.
Güllü, O., Çankaya, M., Biber, M., Türüt, A., 2008c. Gamma irradiation-induced changes at the electrical characteristics of organic-based Schottky structures. J. Phys. D Appl. Phys. 41, 135103.
Gurimskaya, Y., et al., 2020. Radiation damage in p-type EPI silicon pad diodes irradiated with protons and neutrons. Nucl. Instruments Methods Phys. Res. Sect. A Accel. Spectrometers, Detect. Assoc. Equip. 958, 162221.
Hanselaer, P.L., Laflere, W.H., Van Meirhaeghe, R.L., Cardon, F., 1986. The influence of a HF and an annealing treatment on the barrier height of p-and n-type Si MIS structures. Appl. Phys. A 39, 129.
Kaya, A., Marıl, E., Altındal, S., Usluc, I., 2016. The comparative electrical characteristics of Au/n-Si (MS) diodes with and without a 2% graphene cobalt-doped $Ca_3Co_4Ga_{0.001}O_x$ interfacial layer at room temperature. Microelectron. Eng. 149, 166.
Kaymaz, A., Baydilli, E.E., Tecimer, H.U., Altındal, Ş., Azizian-Kalandaragh, Y., 2021. Evaluation of gamma-irradiation effects on the electrical properties of Al/(ZnO-PVA)/p-Si type Schottky diodes using current-voltage measurements,". Radiat. Phys. Chem. 183, 109430.
Krause, O., Ryssel, H., Pichler, P., 2002. Determination of aluminum diffusion parameters in silicon. J. Appl. Phys. 91, 5645–5649.
Lee, Y.H., Wang, K.L., Jaworowski, A., Mooney, P.M., et al., 1980. A transient capacitance study of radiation-induced defects in aluminum-doped silicon. Phys. Status Solidi 57, 697–704.
Lindström, G., Ahmed, M., Albergo, S., Allport, P., Anderson, D., Andricek, L., Angarano, M.M., Augelli, V., Bacchetta, N., Bartalini, P., Bates, R., 2001. Radiation hard silicon detectors—developments by the RD48 (ROSE) collaboration. Nucl. Instrum. Methods Phys. Res. Sect. A Accel. Spectrom. Detect. Assoc. Equip. 466, 308–326.
Missoum, I., Ocak, Y.S., Benhaliliba, M., Benouis, C.E., Chaker, A., 2016. Microelectronic properties of organic Schottky diodes based on MgPc for solar cell applications. Synth. Met. 214, 76–81.
Moloi, S.J., McPherson, M., 2009a. The current and capacitance response of radiation-damaged silicon PIN diodes. Phys. B Condens. Matter 404 (21), 3922–3929.
Moloi, S.J., McPherson, M., 2009b. Current–voltage behaviour of Schottky diodes fabricated on p-type silicon for radiation hard detectors. Physica B: Condense Matter 404, 2251.
Nevin, J.H., Henderson, H.T., 1975. Thallium-doped silicon ionization and excitation levels by infrared absorption. J. Appl. Phys. 46, 2130–2133.
Parida, M.K., Sundari, S.T., Sathia Moorthy, V., Sivakumar, S., 2018. Current–voltage characteristics of silicon PIN diodes irradiated in KAMINI nuclear reactor. Nucl. Instrum. Methods Phys. Res. 568, 7129–7137.
Rajan, L., Periasamy, C., Sahula, V., 2016. Electrical characterization of Au/ZnO thin film Schottky diode on silicon substrate. Perspectives in Science 8, 66–68.
Reddy, V.R., Reddy, N.N., 2012. Current transport mechanisms in Ru/Pd/n-GaN Schottky barrier diodes and deep level defect studies. Superlattice. Microst. 52, 484.
Rosenfeld, A.B., 2006. *Semiconductor Detectors in Radiation Medicine: Radiotherapy and Related Applications Radiation Detectors for Medical Applications* (NATO Security through Science Series). Springer, Dordrecht, pp. 111–147.
Rosenits, P., Roth, T., Glunz, S.W., Beljakowa, S., 2007. Determining the defect parameters of the deep aluminium-related defect center in silicon. Appl. Phys. Lett. 91, 122109.
Sevgili, Ö., 2021. On the examination of temperature-dependent possible current-conduction mechanisms of Au/(nanocarbon-PVP)/n-Si Schottky barrier diodes in wide range of voltage. J. Mater. Sci. Mater. Electron. 32, 10112.
Song, J.O., Leem, D.S., Kwak, J.S., Nam, O.H., Park, Y., Seong, T.Y., 2003. Low-resistance and highly-reflective Zn–Ni solid solution/Ag ohmic contacts for flip-chip light-emitting diodes. Appl. Phys. Lett. 83, 4990–4992.
Sze, S.M., Li, Y., Ng, K.K., 2021. Physics of Semiconductor Devices. John wiley & sons.
Terzo, S., et al., 2017. Radiation hard silicon particle detectors for HL-LHC—RD50 status report. Nucl. Instrum. Methods Phys. Res. 845, 177–180.
Thebe, M.J., Moloi, S.J., Msimanga, M., 2021. Changes in electrical properties and conduction mechanisms of Pd/n-Si diodes due to niobium dopant. Mater. Sci. Eng., B 273, 115392.
Tian, J., Cao, G., 2016. Design, fabrication and modification of metal oxide semiconductor for improving conversion efficiency of excitonic solar cells. Coord. Chem. Rev. 320, 193.
Van Lint, V.A., 1987. The physics of radiation damage in particle detectors. Nucl. Instrum. Methods Phys. Res. Sect. A Accel. Spectrom. Detect. Assoc. Equip. 253 (3), 453–459.
Vittone, E., Olivero, P., Nava, F., Manfredotti, C., Giudice, A.L., Fizzotti, F., Egeni, G., 2005. Lateral IBIC analysis of GaAs Schottky diodes. Nucl. Instrum. Methods Phys. Res. Sect. B Beam Interact. Mater. Atoms 231, 513–517.
Yüksel, Ö.F., Ocak, S.B., Selçuk, A.B., 2008. High frequency characteristics of tin oxide thin films on Si. Vacuum 82, 1183–1186.